Influence of Mixed Sulfur–Nitrogen Oxides on the Redox Kinetics of Manganese Ions in Aqueous Solution

Frans F. Prinsloo,[a,b] **Jakobus J. Pienaar,**[a,b] **Rudi van Eldik***[,a] **and Heinz Gutberlet**[c]
[a] *Institute for Inorganic Chemistry, University of Witten/Herdecke, 58448 Witten, Germany*
[b] *Department of Chemistry, Potchefstroom University Potchefstroom 2520, South Africa*
[c] *VEBA Kraftwerke Ruhr AG, 45801 Gelsenkirchen, Germany*

The influence of mixed sulfur–nitrogen oxides on the redox behaviour of manganese(II,III) species in aqueous solution was studied kinetically as a function of various concentrations and temperature. A series of oxides were found to reduce Mn^{III} to Mn^{II}, whereby these oxides undergo a Mn^{III}-induced hydrolysis reaction. The hydrolysis products were analysed by ion chromatography. These redox reactions can account for the inhibiting effect of the oxides on the metal-catalysed autoxidation of sulfur(IV) oxides in flue gas desulfurization systems. Possible reaction mechanisms are suggested.

Recent studies in our laboratories have focused on the interaction of sulfur and nitrogen oxides with metal ions and complexes in order to contribute towards a better understanding of the role of metal-catalysed autoxidation reactions of these species in atmospheric water droplets. Our work on sulfur(IV) oxides, *i.e.* HSO_3^- and SO_3^{2-}, clearly demonstrated the important role of redox cycling of the catalytic species, *viz.* $Fe^{II,III}$ and $Mn^{II,III}$, during the autoxidation process.[1–7] Similar effects have now also been reported by other laboratories.[8,9] In the case of nitrogen oxides, *i.e.* mainly NO, NO_2^- and HNO_2, iron(II) ions and complexes play a crucial role in their redox chemistry, which again involves redox cycling of the iron(II,III) system.[7,10,11]

The above-mentioned oxides of S^{IV} and $N^{II,III}$ undergo a series of reactions in aqueous solution to produce a range of mixed sulfur–nitrogen oxides which exhibit a complicated scheme of reactions, involving the interaction with sulfite, spontaneous and acid-catalysed hydrolysis, and redox reactions, as summarized in Scheme 1.[12–15] The chemistry of these species has been studied by a number of groups,[12–18] and the more recent development of appropriate analytical techniques[19] will assist the further clarification of a number of the suggested reaction steps. The environmental importance of the mixed sulfur–nitrogen oxides, and their eventual influence on atmospheric oxidation processes, are presently unknown and under investigation. However, recent studies have shown that the presence of these oxides can significantly affect the oxidation of sulfur(IV) oxides in flue gas desulfurization (FGD) systems used in coal-fired power plants.[20,21]

In FGD systems, $CaCO_3$, contaminated with metal impurities (Mn, Fe, Pb), is used to precipitate the produced sulfate. The presence of these metal ions is favourable for the metal-catalysed autoxidation of sulfur(IV) oxides, as referred to above, but also results in the contamination of the precipitated $CaSO_4$ with for instance MnO_2. The installation of selective catalysed reduction systems for the removal of NO from flue gases in recent years has led to an inhibition of the overall oxidation process in some FGD systems, which was ascribed to the influence of sulfur–nitrogen oxides.[21,22] Not only are these species present at considerable concentration levels in the scrubber solutions, they are also held partly responsible for the formation of MnO_2 precipitates in the produced $CaSO_4$, and for the inhibition of the overall oxidation process as mentioned above.

We have therefore undertaken a detailed study of the interaction of a series of sulfur–nitrogen oxides with manganese(II,III) species in order to clarify the underlying reaction mechanisms and product distribution. The results of this study show that $ON(SO_3)_3^{3-}$, $HON(SO_3)_2^{2-}$ and $HONH(SO_3)^-$ are the main reactive species involved in determining the redox behaviour of manganese(II,III) species in aqueous solution.

Experimental

Chemicals of analytical reagent grade (Merck and Fluka) and deionized Millipore water were used to prepare all solutions. Argon was used to deaerate solutions where required. Stock solutions of sulfite were prepared daily by dissolving Na_2SO_3 in deaerated water. Other stock solutions were prepared by dissolving NaN_3, $HClO_4$ and HCl (to adjust the pH), $NaClO_4$ (to adjust the ionic strength), $MnCl_2{\cdot}4H_2O$ and $Mn(ClO_4)_2{\cdot}6H_2O$. The ions $ON(SO_3)_3^{3-}$, $HON(SO_3)_2^{2-}$, $HONH(SO_3)^-$ and $HN(SO_3)_2^{2-}$ were synthesised according to literature procedures,[23–27] and their purity was checked by ion chromatography.[19] Eluents for the ion chromatographic work were prepared from sodium carbonate, tetrabutylammonium hydroxide and acetonitrile. Solutions of Mn^{III} were stabilized with an excess of Mn^{II} in either an azide or acetate medium. In the former case a mixture of NaN_3 and $HClO_4$ was used to reach a desired pH, whereas in the latter case $MeCO_2H$ and $Na(O_2CMe)$ were employed. In both cases $Mn(O_2CMe)_3{\cdot}2H_2O$ (Merck) and $Mn(ClO_4)_2{\cdot}6H_2O$ (Fluka) were used as sources for Mn^{III} and Mn^{II}, respectively.

The UV/VIS spectra were recorded on a HP 8452A diode-array spectrophotometer. Kinetic measurements were performed in the thermostatted cell compartment of the spectrophotometer for slow reactions and on a Durrum D110 stopped-flow instrument for fast reactions. Both instruments were interfaced with an IBM compatible personal computer and data fitting was performed with the OLIS KINFIT (Bogart, GA) set of programs. pH Measurements were performed on a Metrohm 632 pH meter equipped with a Sigma glass electrode. A Metrohm SM-Titrino 702 titration unit was used for the successive addition of small volumes of reagents to a reaction mixture under well controlled pH and temperature conditions. Details of the ion-chromatographic procedures and equipment used are given elsewhere.[19]

Results and Discussion

General Considerations and Observations.—It was the main goal of this study to investigate the redox behaviour of manganese(II,III) species in the presence of a series of sulfur–nitrogen oxides and at the same time identify the decomposition

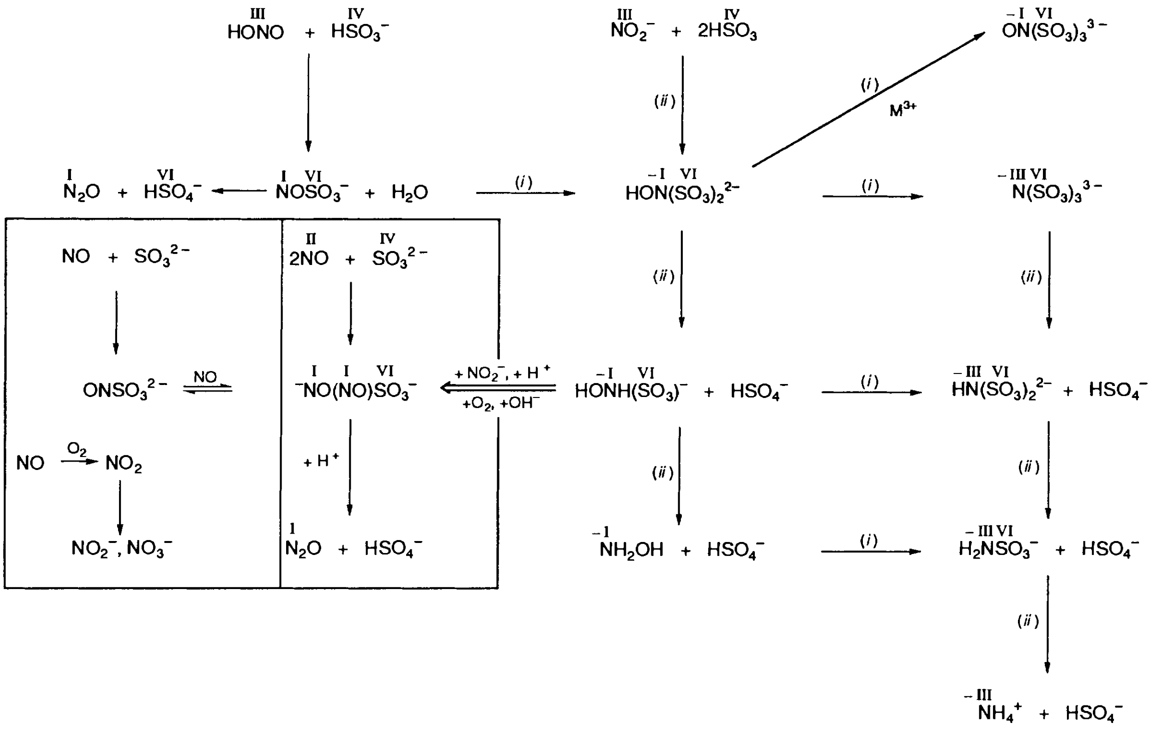

Scheme 1 Formation and hydrolysis reactions of nitrogen–sulfur compounds. (i) HSO_3^-; (ii) H_2O, H^+

products of the oxides under such conditions. For this reason it was essential to select experimental conditions which allowed the stabilization of manganese(III) species to some degree in order to be able to study their interaction with the oxides. Aquated manganese(III) species can only be stabilized in acidic solution in the presence of a large excess of Mn^{II} which prevents the disproportionation of Mn^{III} to Mn^{IV} and Mn^{II}.[28] Furthermore, it is known that the investigated oxides undergo acid-catalysed hydrolysis reactions, which restricts the present investigation to the range $pH > 3$.[19,29–34] Under these conditions Mn^{III} can only be stabilized in the presence of complexing reagents, which has been done in studies using Mn^{III} to oxidize inorganic and organic materials.[35–40] Based on our earlier experience[5,41] and the excellent properties of azide to form stable metal complexes[42,43] we used this medium to stabilize Mn^{III} under the conditions of this study. By way of comparison, we also used an acetate medium to stabilize Mn^{III} under similar conditions. The instability of manganese(III) solutions at $pH > 9$ (accompanied by the precipitation of MnO_2) and the relative ease of oxidation of Mn^{II} in basic media (which must be present in a large excess to stabilize Mn^{III}) restricted our studies on the reduction of Mn^{III} by sulfur–nitrogen oxides to the range $3 < pH < 6.5$. Under the selected experimental conditions the pH of the test solutions remained constant within ±0.2 units.

Sulfur–nitrogen oxides are in general produced from the interaction of sulfur(IV) oxides with NO, NO_2, HONO and NO_2^-. Their behaviour in aqueous solution can be summarized by the overall Scheme 1, which is based on literature information[12] and our own experience in this area.[19–22,44] Solution acidity strongly affects the distribution of the different oxides, since most undergo acid-catalysed hydrolysis. Formal oxidation states have also been assigned to the oxides in Scheme 1. A summary of the available rate data on their hydrolysis reactions is given in Table 1. From the latter data it follows that the investigated compounds, $HN(SO_3)_2^{2-}$, $HON(SO_3)_2^{2-}$ and $HONH(SO_3)^-$, are relatively stable under the selected experimental conditions ($3 < pH < 6.5$). Experiments in our laboratories indicted that no substantial hydrolysis of $ON(SO_3)_3^{3-}$ occurs at pH 6 over a period of 24 h. We also found that the presence of manganese(II,III) species induced hydrolysis reactions in the range $3 < pH < 6$, which may involve coordination of the oxides to Mn^{III} followed by oxidation of the sulfonate group which induces the hydrolysis process (see further discussion). Typical ion chromatograms[20] recorded in the presence of Mn^{III} indicated that $HON(SO_3)_2^{2-}$ decomposed to $HONH(SO_3)^-$ and sulfate, $ON(SO_3)_3^{3-}$ to $HON(SO_3)_2^{2-}$ and sulfate, whereas $HN(SO_3)_2^{2-}$ decomposed to $H_2NSO_3^-$ and sulfate. No other products than those usually found during acid hydrolysis could be detected. The products of the reaction of sulfite with Mn^{III} were found to be sulfate and dithionate. It is important to note that the Mn^{III}-induced hydrolyses do not correspond to a stoichiometric reaction with the oxides. The conversion of the oxides into their hydrolysis products is *ca.* 10^2

Table 1 Summary of hydrolysis rate constants as a function of pH for several sulfur–nitrogen oxides[27–34]

Compound	pH	T/°C	k/s^{-1}
$HON(SO_3)_2^{2-}$	6.4	25	5.0×10^{-9}
	5		3.7×10^{-8}
	4		3.7×10^{-7}
	3		3.7×10^{-6}
	2		3.7×10^{-5}
	1		3.6×10^{-4}
$HONH(SO_3)^-$	6.4	75	6.7×10^{-7}
	3.2		2.0×10^{-6}
	1.6		7.0×10^{-6}
	1.3		1.6×10^{-5}
	1		2.7×10^{-5}
$N(SO_3)_3^{3-}$	5.8	25	5×10^{-5}
	3.9		1×10^{-3}
	2.7		1×10^{-2}
	2.0		2×10^{-2}
$HN(SO_3)_2^{2-}$	1.8	25	1×10^{-2}
	2.0		9×10^{-3}

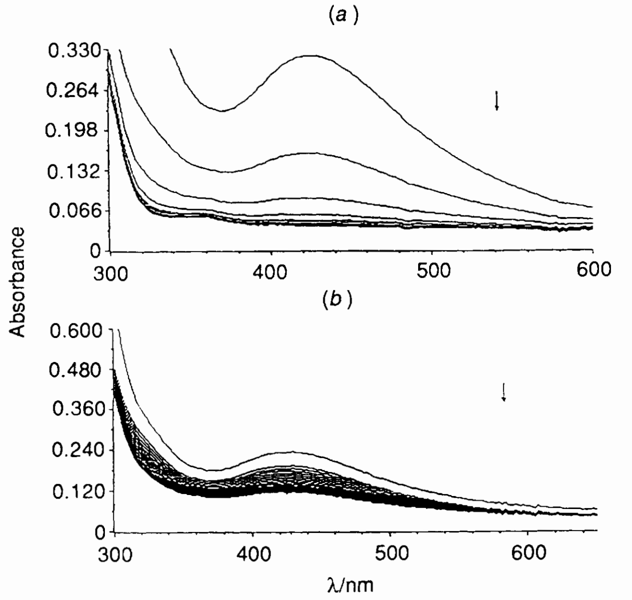

Fig. 1 Reduction of $[Mn(N_3)]^{2+}$. Experimental conditions: $[Mn^{III}] = 4 \times 10^{-5}$, $[Mn^{II}] = 0.1$ mol dm^{-3}; pH 5.5; $[\text{azide}]_T = 0.25$ mol dm^{-3}; $I = 0.5$ mol dm^{-3}; argon-saturated solutions; $\Delta t = 10$ s (*a*) $[HONH(SO_3)^-]_T = 1 \times 10^{-5}$ mol dm^{-3}, 10 °C; (*b*) $[HON(SO_3)_2{}^{2-}]_T = 2 \times 10^{-4}$ mol dm^{-3}, 25 °C

times higher than the manganese(III) concentration employed, which clearly points to a catalytic role of $Mn^{II,III}$ in such hydrolysis reactions.

Reduction of Mn^{III} *by Sulfur–Nitrogen Oxides.*—According to the available stability constant data,[45,46] Mn^{II} produces 1 : 1, 1 : 2, 1 : 3 and 1 : 4 complexes with N_3^-, for which $\beta_1 = 4.15$ mol dm^{-3}, $\beta_2 = 6.61$ mol^2 dm^{-6}, $\beta_3 = 3.35$ mol^3 dm^{-9} and $\beta_4 = 0.64$ mol^4 dm^{-12} at 25 °C and 2.0 mol dm^{-3} ionic strength, whereas Mn^{III} only produces a 1 : 1 complex with N_3^- ($\beta_1 = 82 \pm 20$ mol dm^{-3}) in the range $[N_3^-]$ 0–1.8 mol dm^{-3} at 25 °C and 2.0 mol dm^{-3} ionic strength. Manganese(III) in azide or acetate medium is characterized by an absorbance maximum at 420 nm. On the addition of $HON(SO_3)_2{}^{2-}$, $ON(SO_3)_3{}^{3-}$, $HONH(SO_3)^-$ and $HN(SO_3)_2{}^{2-}$ to a solution containing Mn^{III} in the presence of Mn^{II} and azide a rapid decrease in the manganese(III) concentration is observed as shown for two cases in Fig. 1. In most cases the reactions exhibit simple first-order decay kinetics and the observed rate constant, k_{obs}, varies linearly with the concentration of the sulfur–nitrogen oxide. Some typical results are shown in Fig. 2 for the reduction of Mn^{III} by these four anions at pH 4.5 and 6.5. Some complications were observed under other conditions. For instance the reaction with $HN(SO_3)_2{}^{2-}$ exhibits two consecutive reaction steps at pH 6.5 (Fig. 3), and similarly for $ON(SO_3)_3{}^{3-}$ at pH 5.5 (Fig. 4). In the case of $HN(SO_3)_2{}^{2-}$ the first step depends on the anion concentration but the second step is concentration independent. In the case of $ON(SO_3)_3{}^{3-}$ both reaction steps are independent of its concentration under these conditions. The kinetic results are summarized in Table 2, linear concentration dependences being expressed as in equation (1).

$$k_{obs} = k_1[\text{oxide}] \qquad (1)$$

By way of comparison we recorded kinetic data for the reduction of Mn^{III} by HSO_3^- under similar conditions. Once again two subsequent exponential decays were observed (see Fig. 5), for which both rate constants exhibited a non-linear dependence on the $[S^{IV}]_T$ as shown in Fig. 6. The data can be fitted with the rate equation (2) as demonstrated by the plots of $k_{obs}/[S^{IV}]_T$ *versus* $[S^{IV}]_T$ shown in Fig. 7. A non-linear least-squares fit of the experimental data according to equation (2) results in the k_1 and k_2 values summarized in Table 3.

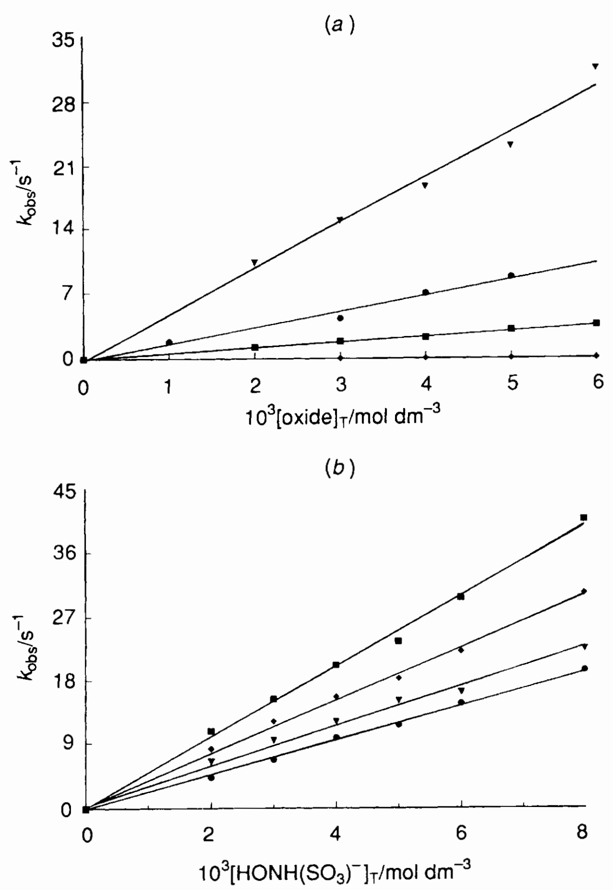

Fig. 2 Plots of first-order rate constants *versus* $[\text{oxide}]_T$. Experimental conditions: $[Mn^{III}] = 4 \times 10^{-5}$, $[Mn^{II}] = 0.1$, $[\text{azide}]_T = 0.25$ mol dm^{-3}; $I = 0.5$ mol dm^{-3}. (*a*) Plots for different oxides (25 °C, pH 6.5): $ON(SO_3)_3{}^{3-}$ (●), $HN(SO_3)_2{}^{2-}$ (◆), $HON(SO_3)_2{}^{2-}$ (■) and $HONH(SO_3)^-$ (▼). (*b*) Temperature dependence for the reaction with $HONH(SO_3)^-$ (pH 4.5): 20 (●), 25 (▼), 30 (◆) and 35 °C (■)

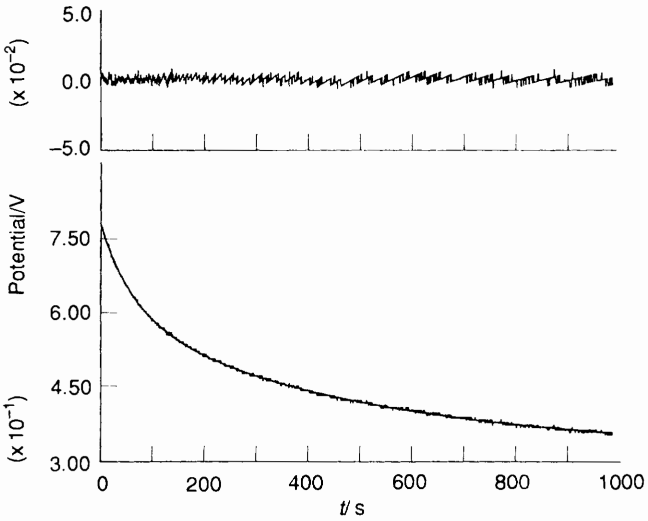

Fig. 3 Absorbance *vs.* time trace for the reaction of $HN(SO_3)_2{}^{2-}$ with $[Mn(N_3)]^{2+}$. Experimental conditions: $[Mn^{III}] = 4 \times 10^{-5}$, $[Mn^{II}] = 0.1$, $[HN(SO_3)_2{}^{2-}]_T = 3 \times 10^{-3}$, $[\text{azide}]_T = 0.25$ mol dm^{-3}; $I = 0.5$ mol dm^3; 25 °C; pH 6.5; λ = 400 nm; 10 V = 1 absorbance unit

The results in Tables 2 and 3 also indicate that in general the reduction of Mn^{III} proceeds faster at higher pH and at lower azide concentration, which must be related to the change in speciation which is controlled by these factors. In general the deprotonation of aquated metal ions will lead to more sub-

Table 2 Summary of kinetic data for the reduction of Mn^{III} by different sulfur–nitrogen oxides in 0.25 mol dm^{-3} azide[a]

Oxide	pH	T/°C	[Oxide]/mol dm^{-3}	k_1[b]/dm^3 mol^{-1} s^{-1}
$HON(SO_3)_2^{2-}$	5.5	25.0	$(1-6) \times 10^{-3}$	298 ± 7
	6.5	25.0	$(2-6) \times 10^{-3}$	605 ± 9
$HONH(SO_3)^-$	4.5	20.0	$(2-8) \times 10^{-3}$	$(2.4 \pm 0.1) \times 10^3$
		25.0		$(2.7 \pm 0.1) \times 10^3$
		30.0		$(3.7 \pm 0.1) \times 10^3$
		35.0		$(5.0 \pm 0.1) \times 10^3$
	5.5	25.0	$(2-6) \times 10^{-3}$	$(2.9 \pm 0.1) \times 10^3$
	6.5	25.0	$(2-6) \times 10^{-3}$	$(5.1 \pm 0.3) \times 10^3$
$HN(SO_3)_2^{2-}$	6.5	25.0	$(3-7) \times 10^{-3}$	5.49 ± 0.17 $(2.0 \pm 0.2) \times 10^{-3}$[c]
$ON(SO_3)_3^{3-}$	5.5	25.0	$(2-5) \times 10^{-3}$	2.0 ± 0.2[d] 0.42 ± 0.04[c]
	6.5	25.0	$(1-5) \times 10^{-3}$	$(1.72 \pm 0.07) \times 10^3$

[a] Experimental conditions: $[Mn^{III}] = 4 \times 10^{-5}$, $[Mn^{II}] = 0.1$ mol dm^{-3}; $420 < \lambda < 500$ nm; ionic strength = 0.5 mol dm^{-3}. [b] Calculated from the slope of a plot of k_{obs} *versus* [oxide] as shown in Fig. 2 unless otherwise indicated. [c] Second reaction step independent of [oxide] and reported as the mean first-order rate constant in s^{-1}. [d] First reaction step independent of [oxide] and reported as the mean first-order rate constant in s^{-1}.

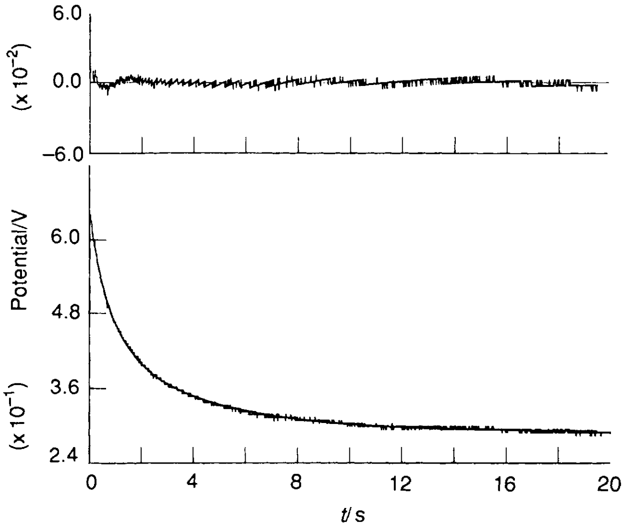

Fig. 4 Absorbance *vs.* time trace for the reaction of $ON(SO_3)_3^{3-}$ with $[Mn(N_3)]^{2+}$. Experimental conditions as in Fig. 3 except $[ON(SO_3)_3^{3-}]_T = 4 \times 10^{-3}$ mol dm^{-3} and pH 5.5

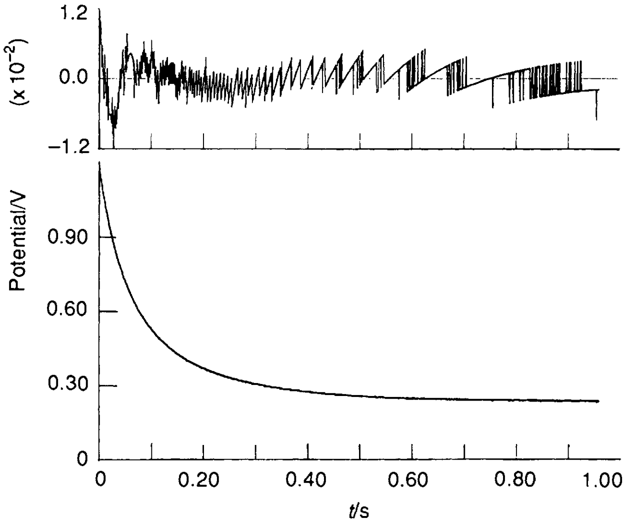

Fig. 5 Absorbance *vs.* time trace for the reaction of sulfite with $[Mn(N_3)]^{2+}$. Experimental conditions as in Fig. 3 except $[sulfite]_T = 1 \times 10^{-3}$ mol dm^{-3} and pH 4.5

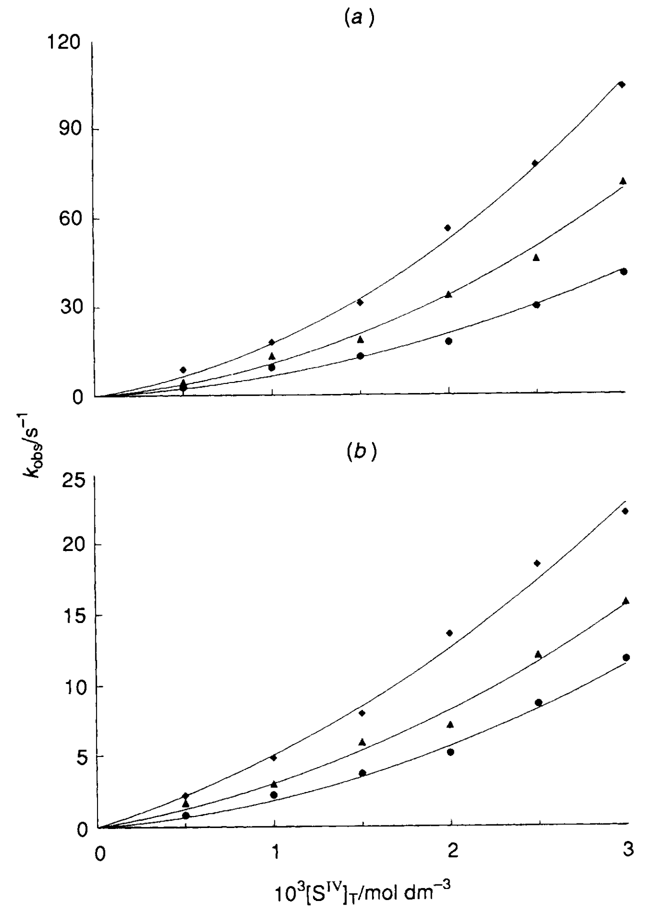

Fig. 6 Plots of first-order rate constants *versus* $[sulfite]_T$. Experimental conditions: $[Mn^{III}] = 4 \times 10^{-5}$, $[Mn^{II}] = 0.1$, $[azide]_T = 0.25$ mol dm^{-3}; $I = 0.5$ mol dm^{-3}; 25 °C. (*a*) First reaction step, (*b*) second reaction step at 20 (●), 25 (▲) and 30 °C (◆)

stitution-labile hydroxo species due to the *trans*-labilization effect of co-ordinated hydroxide. An increase in $[H^+]$ will cause a protonation of SO_3^{2-} to HSO_3^-, which could slow down the redox reaction, whereas an increase in $[N_3^-]$ will cause a stabilization of the manganese(III) species and a lower redox rate.

The different dependences of k_{obs} on [oxide] and $[S^{IV}]$ reported above must be related to the nature of the rate-

Table 3 Summary of kinetic data for the reduction of Mn^{III} by sulfur(IV) oxides in azide media[a]

pH	T/°C	$[N_3^-]$/ mol dm^{-3}	Reaction step	k_1[b]/ dm^3 mol^{-1} s^{-1}	$10^{-6}k_2$[b]/ dm^6 mol^{-2} s^{-1}
4.5	20.0	0.25	1	$(2.6 \pm 1.9) \times 10^3$	3.8 ± 0.8
			2	$(8.1 \pm 3.8) \times 10^2$	1.0 ± 1.5
	25.0		1	$(4.2 \pm 2.5) \times 10^3$	6.3 ± 1.0
			2	$(1.9 \pm 0.5) \times 10^3$	1.1 ± 0.2
	30.0		1	$(8.3 \pm 2.9) \times 10^3$	8.9 ± 1.2
			2	$(3.7 \pm 0.8) \times 10^3$	1.3 ± 0.2
5.5	25.0	0.25	1	$(7.2 \pm 1.0) \times 10^3$	2.1 ± 0.4
			2	$(2.3 \pm 0.2) \times 10^3$	1.8 ± 0.6
5.5	25.0	0.5	1	206 ± 15[c]	

[a] Experimental conditions: $[Mn^{III}] = 4 \times 10^{-5}$, $[Mn^{II}] = 0.1$ mol dm^{-3}; $420 < \lambda < 500$ nm; $[S^{IV}] = (0.5\text{–}3) \times 10^{-3}$ mol dm^{-3}; ionic strength = 0.5 mol dm^{-3}. [b] Determined from the plots in Fig. 7 according to equation (2). [c] Plot of k_{obs} *versus* $[S^{IV}]$ exhibits an intercept of 0.22 ± 0.03 s^{-1} under these conditions.

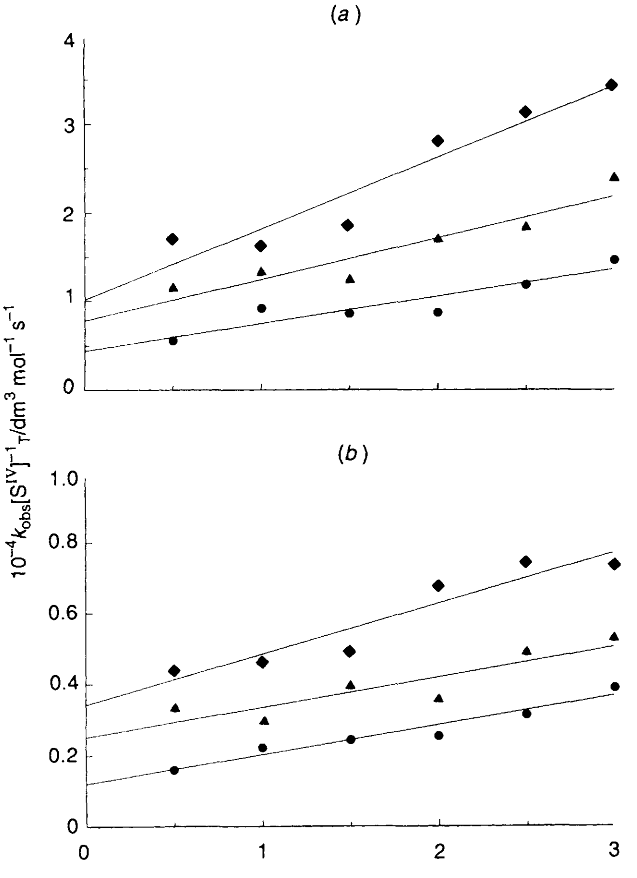

Fig. 7 Plots of $k_{obs}/[S^{IV}]_T$ *versus* $[S^{IV}]_T$. Experimental conditions as in Fig. 6

determining step of the redox reaction. In the case of $ON(SO_3)_3^{3-}$ the independence of k_{obs} on $[ON(SO_3)_3]^{3-}$ for both reaction steps observed at pH 5.5 may either be due to a rate-determining dissociation of a co-ordinated water molecule on the manganese(III) species, or a slow intramolecular electron-transfer reaction following the rapid formation of a Mn^{III}–$ON(SO_3)_3^{3-}$ complex. The two reaction steps observed may involve $[Mn(H_2O)_6]^{3+}$ and $[Mn(H_2O)_5(N_3)]^{2+}$, respectively,[46] for which the speciation is controlled by $[N_3^-]$. Azide is known to stabilize the manganese(III) state, such that it is reasonable to expect that $[Mn(H_2O)_6]^{3+}$, or its deprotonated analogues, is more readily reduced by the sulfur–nitrogen and sulfur(IV) species than is $[Mn(H_2O)_5(N_3)]^{2+}$, or its deprotonated analogues. Although the exact speciation of the deprotonated (hydroxo) species is unknown, it is safe to assume that appreciable deprotonation of the aqua complexes will occur under the selected experimental conditions. A similar explanation can account for the two reaction steps observed for the reduction of Mn^{III} by sulfite. The linear concentration dependence of k_{obs} on [oxide] in equation (1) was found for most of the oxides, and indicates that the redox process can follow either an inner- or outer-sphere electron-transfer mechanism. The high substitution lability of aquated manganese(III) species would favour the operation of an inner-sphere mechanism. This will even be more favoured by the formation of mixed aqua–hydroxo species, since these are generally known to be significantly more labile (due to *trans*-labilization by co-ordinated hydroxide) than are the corresponding aqua complexes. The $[S^{IV}]$ dependence described by equation (2) suggests that 1 : 1 and 1 : 2 Mn^{III}–sulfite species participate in the redox process, where the 1 : 2 species is especially formed at higher sulfite concentrations, presumably from the 1 : 1 species. Thus a plausible mechanism for the reaction with hydrogensulfite can be summarized as in Scheme 2. For simplicity, no hydroxo complexes are included although they are very likely to be the more reactive species as outlined above. Similar reactions will occur with sulfite. The sulfite radicals produced can react with another manganese(III) species to produce Mn^{II} and sulfate, or in the presence of oxygen induce the autoxidation of Mn^{II} to Mn^{III} *via* the formation of $^{\cdot}SO_5^-$.[5]

$$[Mn(H_2O)_6]^{3+} + N_3^- \rightleftharpoons [Mn(H_2O)_5(N_3)]^{2+} + H_2O$$

$$[Mn(H_2O)_6]^{3+} + HSO_3^- \rightleftharpoons [Mn(H_2O)_5(SO_3)]^{+} + H_3O^+$$

$$[Mn(H_2O)_5(SO_3)]^{+} + HSO_3^- \rightleftharpoons \textit{trans-}[Mn(H_2O)_4(SO_3)_2]^- + H_3O^+$$

$$[Mn(H_2O)_5(N_3)]^{2+} + HSO_3^- \rightleftharpoons \textit{trans-}[Mn(H_2O)_4(N_3)(SO_3)] + H_3O^+$$

$$\textit{trans-}[Mn(H_2O)_4(N_3)(SO_3)] + HSO_3^- \rightleftharpoons \textit{trans-}[Mn(H_2O)_4(SO_3)_2]^- + HN_3$$

$$[Mn(H_2O)_5(SO_3)]^{+} \xrightarrow{\text{fast}} Mn^{2+}(aq) + {}^{\cdot}SO_3^-$$

$$\textit{trans-}[Mn(H_2O)_4(SO_3)_2]^- \xrightarrow{\text{fast}} Mn^{2+}(aq) + SO_3^{2-} + {}^{\cdot}SO_3^-$$

$$\textit{trans-}[Mn(H_2O)_4(N_3)(SO_3)] \xrightarrow{\text{fast}} Mn^{2+}(aq) + N_3^- + {}^{\cdot}SO_3^-$$

Scheme 2

A similar reaction sequence can account for the linear concentration dependence observed for the reactions with

Table 4 Activation parameters for the reduction of Mn^{III} by HSO_3^- and $HONH(SO_3)^-$ *

Species	Reaction step	Rate constant	$\Delta H^‡$/ kJ mol^{-1}	$\Delta S^‡$/ JK^{-1} mol^{-1}
HSO_3^-	1	k_1	85 ± 10	+106 ± 34
		k_2	59 ± 6	+8 ± 19
	2	k_1	110 ± 6	+186 ± 20
		k_2	18 ± 2	−70 ± 6
$HONH(SO_3)^-$	1	k_1	35 ± 5	−60 ± 17

* For experimental conditions see Tables 2 and 3.

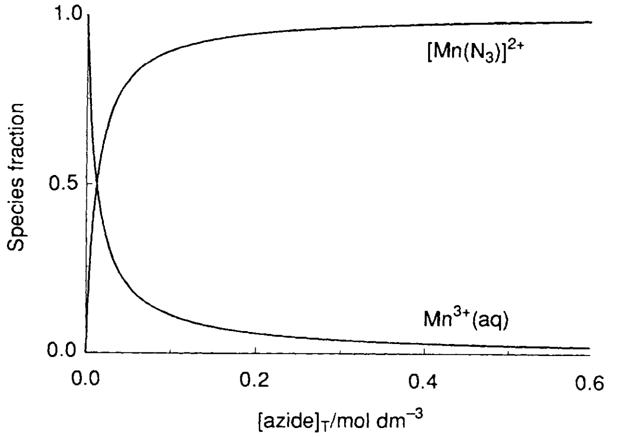

Fig. 8 Speciation of manganese(III) as a function of azide concentration

$HON(SO_3)_2^{2-}$, $HONH(SO_3)^-$ and $HN(SO_3)_2^{2-}$ under all conditions, with $[Mn(H_2O)_6]^{3+}$, or its deprotonated analogues, probably being the most reactive species. A comparison of the values of k_1 in Tables 2 and 3 suggests the following reactivity order SO_3^{2-} > $HONH(SO_3)^-$ > $ON(SO_3)_3^{3-}$ > $HON(SO_3)_2^{2-}$ > $HN(SO_3)_2^{2-}$ at pH 6.5. It follows that HSO_3^- and $HONH(SO_3)^-$ are the most effective reducing agents for Mn^{III} at this pH. At pH 5.5 $HON(SO_3)_2^{2-}$ is more reactive than $ON(SO_3)_3^{3-}$, although HSO_3^- and $HONH(SO_3)^-$ are again the most reactive reducing agents. The redox reactions will result in partial or complete oxidation of sulfite (see further discussion), which will involve the formation of $^{\bullet}SO_3^-$ radicals. These species are essential for the autoxidation of the reduced metal ions.[5] The activation parameters reported in Table 4 allow an extrapolation of the measured rate constants to other temperatures for the two strongest reducing agents, but do not reveal any further mechanistic information since they represent composite quantities as can be seen from the suggested mechanism in Scheme 2.

A crucial aspect of this study is the complex-formation reaction with N_3^- to control the stability of the manganese(III) species. The stability constant reported for the $Mn(N_3)^{2+}$ species[46] is 89 ± 18 (spectrophotometric determination) and 74 ± 15 dm^3 mol^{-1} (kinetic determination). These values result in the speciation curves shown in Fig. 8, from which it follows that at 0.25 mol dm^{-3} *ca.* 5% of the total Mn^{III} is in the Mn^{3+}(aq) form, whereas at 0.5 mol dm^{-3} N_3^- this fraction has reduced to *ca.* 2%. Rather similar results were also obtained in acetate media as indicated by the data in Table 5. Under the selected conditions Mn^{III} was not reduced by $ON(SO_3)_3^{3-}$ and $HN(SO_3)_2^{2-}$, whereas the other three species exhibit the reactivity pattern HSO_3^- > $HONH(SO_3)^-$ > $HON(SO_3)_2^{2-}$ similar to that observed in azide media at significantly higher pH. From this we conclude that our data in azide media can be used to predict the behaviour of sulfur–nitrogen oxides in the presence of manganese (II,III) species.

Table 5 Kinetic data for the reduction of Mn^{III} by $HON(SO_3)_2^{2-}$, $HONH(SO_3)^-$ and HSO_3^- in acetate media[a]

Oxide	[Oxide]$_T$	k_{obs}[b]/s^{-1}	k_1/dm^3 mol^{-1} s^{-1}
$HON(SO_3)_2^{2-}$	1×10^{-3}	0.11 ± 0.01	103 ± 2
	2×10^{-3}	0.22 ± 0.01	
	3×10^{-3}	0.32 ± 0.01	
	4×10^{-3}	0.40 ± 0.01	
	5×10^{-3}	0.51 ± 0.02	
$HONH(SO_3)^-$	1×10^{-3}	0.59 ± 0.01	470 ± 16
	2×10^{-3}	1.05 ± 0.03	
	3×10^{-3}	1.36 ± 0.02	
	4×10^{-3}	1.89 ± 0.04	
	5×10^{-3}	2.27 ± 0.05	
HSO_3^-	5×10^{-4}	0.72 ± 0.02	784 ± 17
	1×10^{-3}	1.14 ± 0.04	
	1.5×10^{-3}	1.47 ± 0.05	
	2×10^{-3}	1.90 ± 0.05	
	2.5×10^{-3}	2.30 ± 0.04	

[a] Experimental conditions: 25 °C; pH 3; $[MeCO_2H]_T$ = 0.2 mol dm^3; argon-saturated solutions; λ = 500 nm; $[Mn^{III}] = 5 \times 10^{-5}$, $[Mn^{II}]$ = 0.5 mol dm^{-3}; ionic strength = 0.6 mol dm^{-3}. [b] Mean value of at least five kinetic runs.

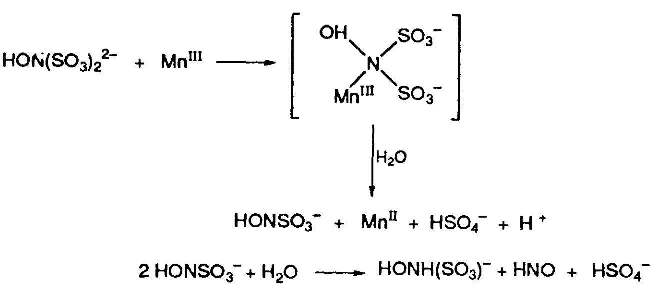

Scheme 3

$$ON(SO_3)_3^{3-} + Mn^{III} + H_2O \longrightarrow Mn^{II} + HSO_4^- + ON(SO_3)_2^{2-} + H^+$$

$$2\,ON(SO_3)_2^{2-} + HSO_3^- \longrightarrow HON(SO_3)_2^{2-} + ON(SO_3)_3^{3-}$$

$$4\,ON(SO_3)_2^{2-} + OH^- \longrightarrow HON(SO_3)_2^{2-} + 2\,ON(SO_3)_3^{3-} + NO_2^-$$

Scheme 4

To what extent do we understand the spontaneous and Mn^{III}-catalysed hydrolysis reactions of the sulfur–nitrogen oxides? During acid catalysis, protonation of the amine will facilitate the hydrolysis reaction, for which a typical example is shown in equation (3). In a similar way Mn^{III} can co-ordinate to the N

$$\begin{array}{c} HON(SO_3)_2^{2-} + H^+ \rightleftharpoons HONH(SO_3)_2^- \\ \big\downarrow{\scriptstyle H_2O} \\ HONH(SO_3)^- + HSO_4^- + H^+ \end{array} \qquad (3)$$

donor atom and induce the hydrolysis process as shown in Scheme 3. In order to complete the catalytic cycle, Mn^{II} can undergo sulfite-induced autoxidation.[5] A similar Scheme (4) can account for the Mn^{III}-catalysed hydrolysis of $ON(SO_3)_3^{3-}$ to $HON(SO_3)_2^{2-}$, which involves the intermediate formation of $ON(SO_3)_2^{2-}$ which undergoes subsequent reactions to $HON(SO_3)_2^{2-}$ and $ON(SO_3)_3^{3-}$. Alternatively, reactions (4) and (5) can account for the formation of $N(SO_3)_3^{3-}$ (ref. 47) *via* the hydrolysis of $ON(SO_3)_3^{3-}$.

$$ON(SO_3)_3^{3-} + Mn^{III} \longrightarrow Mn^{II} + SO_4^{2-} + N(SO_3)_2 \qquad (4)$$

$$2\,N(SO_3)_2 + 3H_2O \longrightarrow N(SO_3)_3^{3-} + HONO + HSO_4^- + 4H^+ \quad (5)$$

The reported kinetic results can account for some of the typical observations made in FGD systems.[20] In plants operating under oxidizing conditions, $N(SO_3)_3^{3-}$ dominates as sulfur–nitrogen oxide in the scrubber solution. Under reducing conditions none of it could be detected. High concentrations of $HON(SO_3)_2^{2-}$ and $HN(SO_3)_2^{2-}$ cause an inhibition of the autoxidation of sulfite, and $ON(SO_3)_3^{3-}$ and $S_2O_6^{2-}$ are present at low concentrations under those conditions. The last two anions are especially produced in cases where not enough oxygen is available for the autoxidation process. The precipitation of MnO_2 is prevented by the presence of $HONH(SO_3)^-$ and $HON(SO_3)_2^{2-}$ since Mn^{III} is effectively reduced by these species. Some laboratory experiments clearly demonstrated that these two ions can prevent the formation of MnO_2 in the presence of Mn^{II}, sulfite and O_2, whereas $HN(SO_3)_2^{2-}$ cannot. Sulfite can induce the autoxidation of Mn^{II} to Mn^{III},[5,7] which will be rapidly reduced by $HONH(SO_3)^-$ and $HON(SO_3)_2^{2-}$ to prevent the formation of MnO_2 *via* the disproportionation of Mn^{III}. No $HONH(SO_3)^-$ could be detected in the FGD systems,[20,21] presumably due to the fact that it is an effective reducing agent for Mn^{III},[47] based on the results of this investigation. The mentioned observations lead to the question as to whether the studied oxides can also induce the autoxidation of Mn^{II} as was found for sulfite.[5,7] This aspect has been studied in more detail and in most cases only seems to play a role at pH > 9. The results will be reported in a forthcoming paper.

Acknowledgements

The authors gratefully acknowledge financial support for this work from VEBA Kraftwerke Ruhr AG, and a stipend from Deutscher Akademischer Austauschdienst to F. F. P. which enabled him to participate in this study.

References

1 J. Kraft and R. van Eldik, *Inorg. Chem.*, 1989, **28**, 2297, 2306.
2 J. Kraft and R. van Eldik, *Atmos. Environ.*, 1989, **23**, 2709.
3 K. Bal Reddy, N. Coichev and R. van Eldik, *J. Chem. Soc., Chem. Commun.*, 1991, 481.
4 K. Bal Reddy and R. van Eldik, *Atmos. Environ.*, 1992, **26**, 661.
5 N. Coichev and R. van Eldik, *Inorg. Chim. Acta*, 1991, **185**, 69.
6 M. Dellert-Ritter and R. van Eldik, *J. Chem. Soc., Dalton Trans.*, 1992, 1037, 1045.
7 N. Coichev and R. van Eldik, *New J. Chem.*, 1994, **18**, 123.
8 J. Berglund, S. Fronaeus and L. I. Elding, *Inorg. Chem.*, 1993, **32**, 4527.
9 J. Ziajka, F. Beer and P. Warneck, *Atmos. Environ.*, in the press.
10 V. Zang, M. Kotowski and R. van Eldick, *Inorg. Chem.*, 1988, **27**, 3279.
11 V. Zang and R. van Eldik, *Inorg. Chem.*, 1990, **29**, 4462.
12 S. G. Chang, D. Littlejohn and N. H. Lin, *ACS Symp. Ser.*, 1982, **188**, 127.
13 D. Littlejohn and S. G. Chang, *Environ. Sci. Technol.*, 1984, **18**, 305.
14 D. Littlejohn and S. G. Chang, *Anal. Chem.*, 1986, **58**, 158.
15 D. Littlejohn, K. J. Hu and S. G. Chang, *Inorg. Chem.*, 1986, **25**, 3131.
16 T. K. Ellison and C. A. Eckert, *J. Phys. Chem.*, 1984, **88**, 2335.
17 L. R. Martin, D. E. Damschen and H. S. Judeikis, *Atmos. Environ.*, 1981, **15**, 191.
18 E. Sada, H. Kumazawa and H. Hikosaka, *Ind. Eng. Chem., Fundam.*, 1984, **23**, 60; 1986, **25**, 386; *Ind. Eng. Chem. Res.*, 1987, **26**, 2016.
19 M. Geißler and R. van Eldik, *Anal. Chem.*, 1992, **64**, 3004.
20 H. Gutberlet, B. Pätsch, R. van Eldik and F. F. Prinsloo, 'Power Plant Chemistry 1993', VGB Conference, Essen, 1993.
21 B. Pätsch, Diplomarbeit, Fachhochschule Gelsenkirchen, 1993.
22 H. Gutberlet, A. Dieckmann and B. Schallert, *VGB Kraftwerkstechnik*, 1991, **71**, 522.
23 V. F. Seele and E. Z. Degener, *Z. Anorg. Allg. Chem.*, 1956, **284**, 101.
24 G. K. Rollefson and C. F. J. Oldershaw, *J. Am. Chem. Soc.*, 1932, **54**, 977.
25 H. Sisler and L. F. Audrieth, *J. Am. Chem. Soc.*, 1938, **60**, 1947.
26 S. Nyholm and L. Rannitt, *Inorg. Synth.*, 1957, **5**, 117.
27 R. Nast, K. Nyul and E. Grziwok, *Z. Anorg. Allg. Chem.*, 1952, **267**, 304.
28 H. Diebler and N. Sutin, *J. Phys. Chem.*, 1964, **68**, 174.
29 J. P. Candlin and R. G. Wilkins, *J. Am. Chem. Soc.*, 1965, **87**, 1490.
30 F. Seel and R. Winkler, *Z. Naturforsch., Teil A*, 1963, **18**, 155.
31 G. J. Doyle and N. Davidson, *J. Am. Chem. Soc.*, 1949, **71**, 3491.
32 M. N. Ackermann and R. E. Powell, *Inorg. Chem.*, 1967, **6**, 1718.
33 D. Littlejohn and S. G. Chang, *Energy Fuels*, 1991, **5**, 249.
34 S. H. Maron and A. R. Berens, *J. Am. Chem. Soc.*, 1950, **72**, 3571.
35 I. K. Bhat, *Transition Met. Chem.*, 1993, **18**, 163.
36 T. E. Jones and R. E. Hamm, *Inorg. Chem.*, 1975, **14**, 1027.
37 P. J. Andrulis, M. J. S. Dewar, R. Dietz and R. L. Hunt, *J. Am. Chem. Soc.*, 1966, **88**, 5473.
38 T. Arantani and M. J. S. Dewar, *J. Am. Chem. Soc.*, 1966, **88**, 5479.
39 P. J. Andrulis and M. J. S. Dewar, *J. Am. Chem. Soc.*, 1966, **88**, 5485.
40 E. I. Heiba, R. M. Dessau and W. J. Koehl, *J. Am Chem. Soc.*, 1969, **91**, 138.
41 N. Coichev and R. van Eldik, *Inorg. Chem.*, 1991, **30**, 2375.
42 M. Monfort, J. Ribas and X. Solans, *J. Chem. Soc., Chem. Commun.*, 1993, 350.
43 L. G. Sillen and A. E. Martell, *Stability Constants of Metal Ion Complexes*, Special Publication No. 17, Royal Society of Chemistry, London, 1989.
44 V. Zang and R. van Eldik, *J. Chem. Soc., Dalton Trans.*, 1993, 111.
45 H. D. Moya, E. F. de Almeida Neves, M. Encarnacion, V. Suarez-Iha and N. Coichev, unpublished work.
46 G. Davies, L. J. Kirschenbaum and K. Kustin, *Inorg. Chem.*, 1969, **8**, 663.
47 *Gmelin Handbuch der anorganischen Chemie*, Gmelin Institute, Frankfurt, 1963, vol. 9, Book no. 5(B), p. 615.

Received 3rd *February* 1994; *Paper* 4/00660G.